

Models for digitally contact-traced epidemics

Chiara Boldrini, Andrea Passarella, and Marco Conti

Abstract—Contacts between people are the absolute drivers of contagious respiratory infections. For this reason, limiting and tracking contacts is a key strategy for the control of the COVID-19 epidemic. Digital contact tracing has been proposed as an automated solution to scale up traditional contact tracing. However, the required penetration of contact tracing apps within a population to achieve a desired target in the control of the epidemic is currently under discussion within the research community. In order to understand the effects of digital contact tracing, several mathematical models have been proposed. In this article, we survey the main ones and we propose a compartmental SEIR model with which it is possible, differently from the models in the related literature, to derive closed-form conditions regarding the control of the epidemic as a function of the contact tracing apps penetration and the testing efficiency. Closed-form conditions are crucial for the understandability of models, and thus for decision makers (including digital contact tracing designers) to correctly assess the dependencies within the epidemic. With our model, we find that digital contact tracing alone can rarely tame an epidemic: for unrestrained COVID-19, this would require a testing turnaround of around 1 day and app uptake above 80% of the population, which are very difficult to achieve in practice. However, digital contact tracing can still be effective if complemented with other mitigation strategies, such as social distancing and mask-wearing.

Index Terms—COVID-19, analytical models, digital contact tracing, testing efficiency

I. INTRODUCTION

SINCE April 2020, the WHO has been recommending two main and complementary strategies for curbing the COVID-19 epidemic: social distancing on the one end, *test, trace, treat* (the famous 3 T’s) on the other. As for any respiratory viral infection, the sooner we are able to “remove” contagious people from interacting with others, the sooner the epidemic will be restrained. Indeed, if, on average, each infected person infects only one susceptible, rather than, e.g., two or three, the epidemic will die down naturally [1]. Of course, for this to be effective, all the three T’s must be carried out swiftly. Contact tracing without testing is impossible: you first have to know that a person is potentially contagious before being able to track down their contacts. Similarly, tracing must be completed as quickly and as thoroughly as possible: the

longest it takes to identify past contacts, the more the time a potentially contagious person spends unknowingly infecting other people. Then, contagious people must be promptly isolated and treated, if needed.

Contact tracing can be performed manually or digitally. Manual contact tracing entails reconstructing the history of the past contacts of the infected person in the days before being detected as contagious. This is typically done through interviews with the infected person. The main problems with manual contact tracing are that i) the contagious person might not be able to recall precisely their past contacts (simply because they forget some or because some chance contacts with strangers are not noticed in the first place), and ii) it does not scale well with the number of daily new cases. Digital contact tracing, performed by means of smartphone apps that – typically via Bluetooth – automatically detect and register contacts, have the potential to overcome the two limitations of manual contact tracing described above. The research community has already identified convincing solutions that provide reasonable trade-offs between privacy and tracing accuracy [2]–[5]. Specifically, decentralised Bluetooth-based contact tracing has emerged as the solution of choice and privacy-preserving apps based on this approach have been deployed in many countries [6]¹ The vast majority of these apps leverage the Exposure Notification protocol jointly rolled out by Apple and Google in Spring 2020. However, digital contact tracing comes with its own problems. The main one is that, for it to be effective, a significant percentage of the population must have the app installed [7]. Bumping up this percentage may not be as easy as it seems [8]. For example, people with old smartphones (typically not supporting Bluetooth Low Energy or for which an updated operating system is not available) cannot enjoy the tracking functionalities. The fear of privacy intrusion by governments turns off other potential participants.

Due to the limitations discussed above, the percentage of people with an installed and fully-functioning contact tracing app will be far from 100%. Thus, key questions are, among others: how large should this percentage be for digital contact tracing to be effective in containing the epidemic? How does this percentage depend on the contact patterns between people? How does it depend on the roll out of other mitigation measures (such as social distancing and mask-wearing)?

The network of people with the contact tracing app installed is just another instance of a mobile social network [9]: people interact with each other socially, and these interactions are mirrored in the data anonymously collected by the contact tracing app. Thus, by leveraging properties of this mobile social network, we will investigate the above problem.

All authors are with CNR-IIT, Via G. Moruzzi 1, 56124, Pisa (e-mail: first.last@iit.cnr.it)

This work was partially funded by the SoBigData++, HumaneAI-Net, and SAI projects. The SoBigData++ and HumaneAI-Net projects have received funding from the European Union’s Horizon 2020 research and innovation programme under grant agreements No 871042 and No 952026, respectively. The SAI project is supported by the CHIST-ERA grant CHIST-ERA-19-XAI-010, funded by MUR (grant No. not yet available), FWF (grant No. I 5205), EPSRC (grant No. EP/V055712/1), NCN (grant No. 2020/02/Y/ST6/00064), ETAg (grant No. SLTAT21096), BNSF (grant No. KP-06-DOO2/5).

This work has been submitted to the IEEE for possible publication. Copyright may be transferred without notice, after which this version may no longer be accessible.

¹For an extensive list: https://en.wikipedia.org/wiki/COVID-19_apps.

Digital contact tracing has yet to be properly evaluated as a public health measure through a large scale assessment [10]. Thus, the answers to the above questions must then necessarily come from mathematical models and simulations. Ferretti *et al.* [7] adapted a model introduced by Fraser *et al.* [1] (and based on the popular Von Foerster equation) in order to provide an initial answer to the question. In this article, in order to complement the model in [7], we propose a deterministic compartmental model for digital contact tracing. The advantage of this modelling approach is that closed form solutions can often be obtained, hence analytical conditions on the control of the epidemic can be derived. *Closed-form control conditions are crucial for the understandability of models and are instrumental for decision makers and computer scientists working on digital contact tracing.* Vice versa, the Von Foerster equation, which is more accurate than simple compartmental models, can only be solved numerically. Alongside the compartmental model, we also introduce a standalone model that captures how the testing delay affects the efficacy of the detection of infected people, depending on the duration of the latent window and the contagious window. This model is general, and can be solved in closed-form for some common distributions describing these time intervals.

The rest of the paper is organised as follows. In Sections II-III, we overview the main results in the related literature regarding COVID-19 modelling and we summarise the properties of the disease itself that are important from the modelling standpoint. Our deterministic compartmental model is presented in Section IV, together with the model on the efficacy of the detection of infected people. The proposed model is then applied to a set of realistic epidemiological scenarios in Section V. Finally, Section VI concludes the paper.

II. A BRIEF OVERVIEW ON COVID-19

From the modelling standpoint, a crucial aspect is to understand when infected people become contagious. For any viral disease, the typical timeline is the following. Following a contact with a contagious person, an individual may become infected. However, they do not become contagious immediately: there is a *latent period* during which the person is infected but not yet contagious (i.e., the virus is replicating but its quantity is not yet enough to infect another person). Another important stage is the *incubation period*, which goes from the infection time to the time when the person starts developing symptoms. The latent period may be shorter than the incubation period: this means that an infected person becomes contagious before developing symptoms. Clearly, this makes controlling the spread of the disease harder, since the contagious person that hasn't developed any symptoms is not aware of their contagiousness. While subject of hot debates in the initial phases of the COVID-19 epidemic, it is now clear that asymptomatic and pre-symptomatic carriers play a major role in the spread of the SARS-CoV-2 virus [11]–[25].

SARS-CoV-2 is an airborne² virus, i.e., it travels through air.

The typical transmission pathway is when a contagious person talks, sneezes, or coughs, producing infectious droplets that are inhaled by the people in close proximity. Less frequently, these droplets may fall on the surfaces in close proximity, and then contribute to transmitting the disease when the contaminated surface is touched by a susceptible person and then this person touches his/her face (eyes, mouth, etc.). The latter transmission pathway is known as environmental transmission. It is not known to play a major role in the COVID-19 epidemic³, hence we will not consider it in the modelling. A third transmission pathway is that of aerosol [26]–[29]: when a contagious person talks, sneezes, or coughs they also produce some smaller droplets (known as aerosol) that evaporate faster than they fall on the ground [30]. This means that with aerosol transmission, the dry virus lingers in the air for considerable time and travels longer distances. The bad news is that common face mask (like the surgical and cloth ones) are not well equipped to contain such small droplets. Thus, aerosol transmission is much more challenging than droplet transmission, that can be easily contained relying on widespread mask-wearing. Model-wise, though, they can be both captured by appropriately tuning the probability of infection upon contact.

III. MODELS OF EPIDEMICS

There are two main modelling approaches in the related literature: mathematical models and agent-based models. Mathematical models of epidemics typically lay out a system of ODE/PDE that describes how the number of susceptibles, infected, etc., vary over time. Sometimes these systems can be solved in closed form and provide very useful trends describing what-if scenarios. Otherwise, numerical solutions can be obtained. Due to their nature, these models are based on several simplifying initial assumptions to make the mathematical representation of the phenomenon tractable. At the opposite side of the modelling spectrum are the agent-based models. Agent-based models are computational models where agents (corresponding to people) interact, in simulation, according to some predefined rules, which can be arbitrarily complex [31]–[37]. They are conceptually very similar to the models used in transportation simulation. They recreate synthetic populations in terms of demographics, traffic flows, etc, then an epidemic is simulated. Since they are not the focus of this work, we will not further discuss them.

By far, the most used mathematical model is the classical SIR model and its many variations [38]. In the basic version, people are divided in three compartments (denoted with S, I, R). In S, people are susceptible to the disease, i.e., they can become infected upon contact with an infectious person. Infectious people are in compartment I. After a certain time spent in compartment I, infected people recover and move to compartment R. Transitions between compartments are then modelled as follows:

²We use the layman's definition of airborne here. The technical use implies only transmission via aerosol.

³<https://www.ecdc.europa.eu/en/covid-19/latest-evidence/transmission>

$$\begin{aligned}\frac{dS}{dt} &= -\beta I \\ \frac{dI}{dt} &= \beta I - \gamma I \\ \frac{dR}{dt} &= \gamma I.\end{aligned}$$

Parameters β and γ describe the rate at which susceptibles become infected and infected recover. The SIR model can be described by a system of Ordinary Differential Equations (ODE) that can be solved in closed form. This representation of an epidemic is referred to as *deterministic*, because the above equations are an approximation, holding for very large populations, of the stochastic version of the SIR model [38]. This simple model has been extended in several directions, adding the *exposed* compartment (where people infected but not yet contagious reside), which we also use in this work, and many more (see [38] for a general discussion and [39] for an application to COVID-19).

The deterministic compartmental models discussed above are based on a simple assumption that the time spent in each compartment can be reasonably approximated with an exponential random variable (the Markovian assumption). When this is not the case, other types of models must be considered. An important class of non-Markovian models are those based on the McKendrick-VonFoerster equation, which incorporates a so-called age structure to the model [38]. Originally, this model was designed to capture births and deaths in the dynamics of population growth in cellular biology: offspring are generated at a young age, death occurs typically at an old age. Hence, keeping track of the population age over time was essential to predict the evolution of the population size. When applied to epidemiology, the *age* is seen from the infection point of view, i.e., it corresponds to the time since the individual became infected. And the *birth rate* at infection age τ becomes the rate at which a person infected τ days ago produces offspring, i.e., new infected people. Thus, the infection rate is not anymore constant over time and it depends on the current age profile of the population.

Finally, a related active area of study for COVID-19 is the correct estimation of the parameters describing the dynamics of the infection [40]–[45]. This is important both for purely mathematical models and for agent-based models, because a correct estimation of the epidemic parameters allows researcher to correctly set up their assumptions and simulations.

IV. FACTORING IN DIGITAL CONTACT TRACING

The McKendrick-VonFoerster model introduced in Sec. III has been used in [7], a seminal paper dedicated to assessing the efficacy of contact tracing for COVID-19. The model by Ferretti *et al.* [7] is based on the one proposed in [1], with parameter values customised to the specific COVID-19 setting. This model is the de-facto reference for digital contact-tracing effectiveness estimation and the vast majority of forecasts, coming both from within the scientific communities and news outlets, have been based on its results. By its own nature, the McKendrick-VonFoerster model can

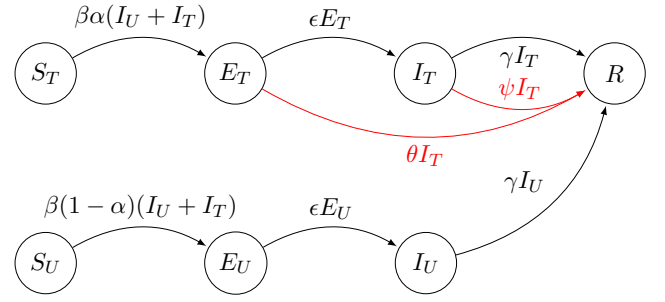


Fig. 1. How people move across SEIR compartments. In red, the arcs associated with containment measures: quarantine of exposed plus isolation of those infected and contagious. α denotes the fraction of digitally tracked population.

only be solved numerically. Hence, it is not able to yield a closed-form condition under which the epidemic can be controlled based on the characteristics of the digital contact tracing process in place. Thus, in this work, we complement the results by Ferretti *et al.* [7] showing that a simpler model, whose control condition is solvable in closed form, can yield the same spreading trends. The notation we use in the paper is summarised in Table I at the end of the section.

We start with a simplified version of the model, presented in Figure 1, for illustrative purposes. As usual for deterministic compartmental models, we start with a population with constant size N , i.e., the sum of the people throughout all states must add up to N . When looking at a large population, the short-term variation of its size is small and can be neglected. The goal of the model is to capture how the infection spreads through the population and to assess whether the spread can be stopped or not by means of digital contact tracing and the resulting quarantine of contacts. We assume that the epidemic is faster than the long-term dynamics of births/deaths in the population, so we ignore the latter. People can be in one of four states: S (*susceptible*), E (*exposed*), I (*infectious*), R (*removed*). Since people can be either tracked (with a contact tracing app) or untracked, we duplicate these states to account for this difference (thus, each state is marked with subscript T or U for tracked and untracked, respectively). We do not need to duplicate the *removed* state because people in R do not contribute to the epidemic anymore. While we use the common letters S , E , I , R to denote the states, we slightly adjust the default meaning of the states to take into account asymptomatic and pre-symptomatic transmission. In this model, then, *exposed* means infected but not yet contagious, while *infectious* means infected and contagious but with no symptoms (this includes the pre-symptomatic and the asymptomatic phase of the disease). The *removed* state includes all infected (whether contagious or not) that have been isolated and/or have recovered. In this simplified model, a person is isolated either because is infected and has been tracked down by the contact tracing app or because she is contagious and has started developing symptoms. We do not include a dedicated state where people are both contagious and symptomatic because it is reasonable to assume that people with symptoms will isolate themselves (hence joining the *removed* state).

The fraction of tracked people is denoted with α , where α represents the percentage of the population that subscribed to the considered contact tracking app. Thus, at time $t = 0$, we have αN people in state S_T (corresponding to people that are susceptible and tracked) and $(1 - \alpha)N$ people in S_U (susceptible but not tracked). From the *susceptible* state, people can only move to the *exposed* state⁴. Recall that “exposed”, in this case, means infected but not yet contagious. Thus, the time spent in the *exposed* state corresponds, without containment measures in place, to the latent period of the disease. However, there is a crucial difference between untracked and tracked exposed: tracked exposed will be notified by health authorities about their past contact with a tracked contagious person and they will be isolated, i.e., they will move to the *removed* state. The same happens for tracked infectious. Removed people are isolated, hence cannot infect anyone. This is the crucial contribution of contact tracing. Below, we summarise how the transitions from each state can be modelled.

$S_U \rightarrow E_U$ The rate at which people leave the S_U state is given by the effective contact rate β (rate at which there is an encounter between an S and an I and this encounter generates an infection) times the number of possible encounters between people in S_U and those in I (we don’t care whether the encounter is with a tracked or untracked infected).

$S_T \rightarrow E_T$ The same holds true for the rate at which tracked susceptibles leave S_T , with the appropriate change from U to T of S’s subscript with respect to the previous case.

$E_U \rightarrow I_U$ Untracked exposed (people in E_U state) stay there until they become contagious, and this happens at a rate ϵ .

$E_T \rightarrow I_T$ Instead, *tracked* exposed will either become contagious and move to state I_T (this happens with rate ϵ) or be warned of having had a contact with an infected and told to self-isolate (this happens with rate θ , discussed in detail in Sec. IV-A).

$I_U \rightarrow R$ Untracked contagious (I_U) are isolated when they start developing symptoms, and this happens at a rate γ .

$I_T \rightarrow R$ Instead, tracked contagious (I_T) can be either isolated when they start developing symptoms (similarly to the untracked case) or be informed of having had a contact with an infected and told to self-isolate (this happens with rate ψ , discussed in detail in Sec. IV-A).

The key point for being able to add the effect of contact tracing to the SEIR equations is to model appropriately the transitions in red in Figure 1. The rates θ and ψ capture how effective digital contact tracing is in removing infected people, and factor in the testing delay as well as the epidemic characteristic features (the latent period, contagious period, etc.). We will discuss this aspect in Section IV-A and we will provide a methodology for deriving θ and ψ . For now, let us assume that we are able to assign proper values to all the parameters of the model. In Theorem 1 below, we discuss how to solve the model and how to assess whether the epidemic

can be controlled or not depending on the efficacy of contact tracing. The proof of the theorem can be found in Appendix A.

Theorem 1. *The epidemic described by the SEIR model in Figure 1 can be controlled when the following condition is true:*

$$C1: \alpha - \left(1 + \frac{\gamma}{\theta + \psi}\right) \left(1 - \frac{\gamma}{\beta}\right) > 0. \quad (1)$$

Remark. The closed-form condition in Theorem 1 could not have been obtained with the model used by Ferretti *et al.* in [7], which can only be solved numerically. Closed-form conditions are crucial for the understandability of models, and thus for decision makers (including digital contact tracing designers) to correctly assess the dependencies within the epidemic.

In order to illustrate the intuition behind condition C1 in Theorem 1, let us consider two ideal cases separately: i) instantaneous tracing ($\theta + \psi \rightarrow \infty$) and ii) perfect app uptake ($\alpha = 1$). These correspond to the two dimensions of digital contact tracing: how good we are in detecting infections of the tracked people and how many people we are able to track. When tracing is instantaneous (corresponding to the first case above), the threshold on α (derived from Equation 1) converges to $1 - \frac{\gamma}{\beta}$. For SIR models, the ratio $\frac{\beta}{\gamma}$ corresponds to the basic reproduction number R_0 [46], hence the threshold on α , interestingly, is equivalent to the herd immunity threshold $1 - \frac{1}{R_0}$. Note that instantaneous tracing alone is not sufficient for controlling the epidemic: α must be high enough for tracking to cover a large fraction of the population. A superfast tracking that only follows just a tiny fraction of the population is basically useless. In the second case (perfect app uptake, i.e. $\alpha = 1$), condition C1 reduces to $\gamma + \theta + \psi > \beta$. Hence, $\theta + \psi$ must be large enough to compensate for a high β (effective contact rate). This means that, even in the ideal condition where everybody has the app ($\alpha = 1$), control of the epidemic may not be attainable if the tracing process is slow. The efficiency of contact tracing is captured by θ and ψ and, in Section IV-A, we discuss how to derive them.

A. Estimating parameter θ and ψ from contact history

We now move one step back and discuss how to model θ and ψ , which are the rates at which exposed and infectious people are removed, respectively. As discussed before, they capture the effectiveness of testing. To derive them, we have to reconstruct the process from contagion (encounter with an infectious person that yields to infection) until removal.

Exposure notifications are triggered by tracked people becoming symptomatic and therefore being tested. We know that, since SEIR models assume homogeneity in encounters (which boils down to a single β describing the entire contact process, with no distinction between high vs low social interactions), the contact rate at which the newly symptomatic tracked person met with tracked susceptibles is $\alpha\beta$ (i.e., the baseline rate scaled by the fraction of tracked people). The above rate must be split across the different states in which the past contact might currently be in. Specifically, a past contact can be still exposed, already infectious, or removed. We neglect the removal of susceptibles because the population of susceptibles is very large (by assumption, $S \sim N$), hence removing them

⁴Technically, some susceptibles can be removed (i.e., asked to isolate) due to, e.g., a faulty detection from the contact tracing app. However, since SEIR models rely on the assumption $S \sim N$, this removal can effectively be ignored.

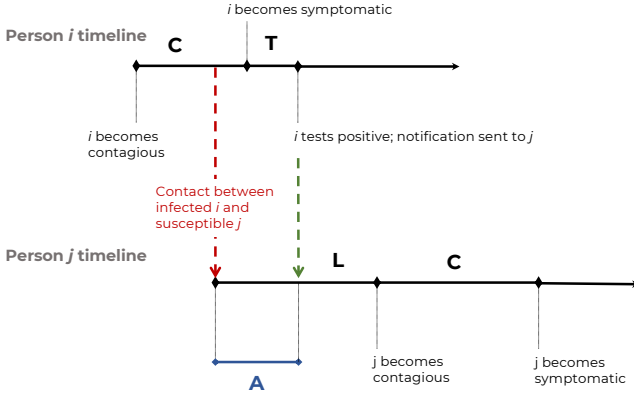


Fig. 2. The timeline of the conversion to symptomatic.

would not impact the epidemic. Thus, Definition 1 below follows.

Definition 1 (Alertable Contacts). *The alertable contacts of a positive person i can be a) in state E_T (no symptoms, not contagious), b) in state I_T (contagious, no symptoms), c) in state R (symptomatic or recovered, hence already “removed” from the epidemic). We denote the probabilities associated with each of these conditions as p_E , p_I , and p_R , respectively (note that they add up to 1).*

Intuitively, health authorities should strive to increase as much as possible p_E , because people in the *exposed* state have yet to infect someone. Of course, this might not be possible (e.g., due to testing delays) so the next best thing is to increase p_I . Instead, notifying people that are already in the *removed* state is completely useless from the epidemic containment standpoint.

As illustrated in Figure 2, we can model the conversion to symptomatic of a past contact considering: the length of the latent period L (which, as discussed in Section II, goes from the time of infection to the time a person becomes contagious), the length of the infectious but asymptomatic period C , and the testing delay T (the time it takes for a test result to be available after the person has developed symptoms). Note that L and C are only determined by the properties of the specific disease. On the contrary, T is totally dependent on the efficacy of the testing system in place, hence it can be shortened by human interventions (e.g., using rapid tests rather than molecular ones or by scaling up testing facilities). The probability distribution of L , C , and T can be obtained from real data, when available (at the end of the section, we will discuss an example based on a realistic duration of the latent and infectious windows). Using their distribution, we can characterise the only missing time interval in Figure 2: A , which represented the time it takes for the app notification to pop up after a contact. In Lemma 1 we derive A ’s distribution.

Lemma 1. *The random variable A describing the time interval between the at-risk contact and the time when the contact tracing app notification arrives is distributed as $C' + T$, i.e., as the sum (between random variables) of the residual infectious-but-asymptomatic period C' and the testing delay T .*

Proof. As illustrated in Figure 2, A describes the time at which

the contact tracing app notification arrives. This time corresponds to the interval between the contact with an infectious person and the notification time, hence it includes a *residual* contagious period (which we denote with C') and the testing delay T . Thus, A is distributed as $C' + T$ (hence its PDF is given by the convolution of the PDF of C' and T [47]). Mathematically, C' can be obtained assuming that the contact between the susceptible and the contagious individuals appears during C as a random observer: as a result, C' can be derived as the residual duration [48] of C for the infectious person i (i.e., the time left before the person becomes symptomatic, hence they are discovered as positive). Denoting with F_X the CCDF of a generic random variable X , the formula for computing the residual time C' is the following [48]:

$$F_{C'}(t) = \frac{1}{E[C]} \int_t^\infty F_C(u) du. \quad (2)$$

Since C can be derived from real epidemic data, C' can be computed as well. \square

Now that A is fully characterised, by deriving its interplay with L and C we obtain p_E , p_I , and p_R in Lemma 2 below.

Lemma 2. *The probabilities p_E , p_I , and p_R (associated, respectively, with catching a person in state E_T , I_T , and R) are given by the following:*

$$\begin{aligned} p_E &= P(W < 0) \\ p_I &= \int_0^\infty P(W = w)P(C > w)dw \\ p_R &= P(W - C > 0), \end{aligned}$$

where we denoted with W the difference $A - L$.

Proof. From Figure 2, we can see that p_E is equivalent to the probability of the notification arriving within the latent period (corresponding to $P(A < L)$). The probability of the notification arriving during the contagious and asymptomatic period ($P(L < A < L + C)$) yields p_I . The value of p_R can then be obtained complementing to 1 (or computing $P(A > L + C)$, i.e., the probability that the notification arrives when the individual is already symptomatic). Operationally, this results in the thesis. \square

Not for all distributions the above algebra of random variables yields closed-form solutions, but for some significant ones it does, at least approximately. This happens, e.g., in the Normal case discussed in the next section (Sec. IV-A1). Closed-form solutions can be also obtained with exponential random variables. Once the probabilities p_E and p_I are derived, it is straightforward to obtain rates θ and ψ .

Theorem 2. *The rates at which exposed and contagious people are removed (θ and ψ , respectively) are given by the following:*

$$\theta = p_E \alpha \beta, \quad (3)$$

$$\psi = p_I \alpha \beta, \quad (4)$$

where p_E and p_I are obtained as in Lemma 2.

Proof. The thesis simply follows from scaling the overall tracked contact rate $\alpha \beta$ by the probability that the exposed

TABLE I
SUMMARY OF NOTATION.

NOTATION	DESCRIPTION
N	population size
S	susceptible population
E	people that have the disease but not yet symptoms
I	contagious & symptomatic people
R	removed people (either recovered or isolated)
$(\)_T$	subscript T denotes compartments that are tracked
$(\)_U$	subscript U denotes compartments that are <i>not</i> tracked
β	effective contact rate
ϵ^{-1}	time from infected to contagious
γ^{-1}	time from contagious to removed (recovery/isolation)
θ	rate at which tracked exposed are isolated
ψ	rate at which tracked infectious are isolated
α	fraction of population with the app installed and running
L	latent period
C	infectious-but-asymptomatic period
T	testing delay
A	time between at-risk contact and app notification
W	time to contagious after app notification
p_E	probability of alerting a person in state E_T
p_I	probability of alerting a person in state I_T
p_R	probability of alerting a person in state R

is notified when still in the *exposed* state or in the *infectious* state. \square

1) *Example with normally distributed characteristic times:* For the sake of example, we can now get p_E , p_I , and p_R leveraging the typical average duration of the latent and contagious periods for the original COVID-19 epidemic. From [49], we obtain the average duration of the latent period ($\mathbb{E}[L] = \epsilon^{-1} = 3$ days) and that of the period before an infected becomes contagious ($\mathbb{E}[C] = \gamma^{-1} = 2$ days). Note that the expectations of L and C correspond to the inverse of ϵ and γ in the SEIR model of Section IV. For example, let us assume that L and C as normally distributed, each with standard deviation 0.5 (the occurrence of negative values with this configuration is negligible). We also assume that T is normally distributed, with rate μ_T and standard deviation σ_T . It is easy to verify that $A = C' + T$ can be approximated as normally distributed as well, specifically $A \sim \mathcal{N}(\mathbb{E}[C'] + \mu_T, \text{Var}(C') + \sigma_T^2)$. Since we are dealing with normally distributed variables, it is easy to obtain their difference and sum using the algebra of normally distributed random variables.

Leveraging the formulas we have obtained, we can now better understand the impact of testing delays on the ability to intercept infected people in each stage using contact tracing. In the following, we focus on a tagged pair of people (one tracked infectious i and one tracked susceptible j infected by i , analogously to Figure 3) and we study the probability that j is notified when in the *exposed*, *infectious*, or *removed* state, respectively, as we vary the testing delay. Note that, since we focus on a tagged pair of tracked people, this result does not depend on α , which is a population-level parameter. As Figure 3 shows, as long as the test turnaround is smaller than 2

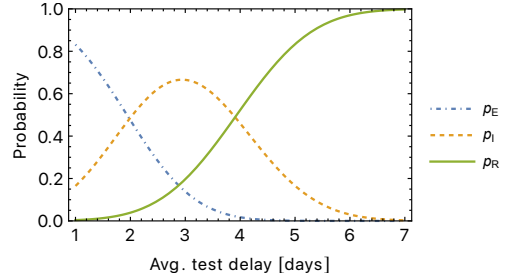


Fig. 3. p_E , p_I , and p_R as the average testing delay increases.

days, the infected person is most likely caught while they are still not contagious. Vice versa, beyond a 4-day turnaround, we basically intercept only people that are already contagious or even symptomatic. As discussed above, the earlier we intercept infected people, the better. Small testing delays are thus a key ingredient of a containment plan.

V. CAN DIGITAL CONTACT TRACING TAME AN EPIDEMIC?

With the derivation of θ and ψ in Section IV-A, our SEIR model is fully characterised. Thus, we can leverage it to study the effectiveness of digital contact tracing in controlling the epidemic. Digital contact tracing is mainly dependent on two parameters: α , the uptake of the app, and the testing delay μ_T . In the following, we will assess their impact on the control condition C1 (Theorem 1) for different epidemic scenarios. In order to solve the model, we need estimates for β (effective contact rate), γ (transition rate to symptomatic), and ϵ (transition rate to contagious). For epidemics, γ and the ratio $\frac{\beta}{\gamma}$, corresponding to the basic reproduction number R_0 , are typically estimated. Hence, in the following, β will be set to the value yielding the COVID-19 R_0 for the chosen γ . Intuitively, the basic reproduction number R_0 captures the average number of cases directly generated by one infectious person in a population with a very large number of susceptibles. As we also see below, the larger R_0 , the more difficult the containment of the epidemic with digital contact tracing (and in general).

We start (Figure 4) with a scenario with an average contagious but asymptomatic window length (γ^{-1}) equal to 2 days (typical of COVID-19) and fixed $R_0 = 2$ (this value correspond to the initial 2020 estimate for COVID-19 in [7]). We test the effect of an increasing latent period length ($\epsilon^{-1} \in \{1, 3, 5\}$ days) on the controllability. Specifically, we plot the condition C1 in Equation 1 as a function of the app uptake α and the testing delay: the epidemic is tamed in the shadowed areas of the plot. Intuitively, the longer the latent period, the more feasible is the control of the epidemic, because we have more time to intercept tracked people before they become contagious. Figure 4 confirms this: as ϵ^{-1} increases, the importance of small testing delays is reduced, we just need more than 80% of people with the app installed. Technically, an increase in ϵ^{-1} induces a temporal shift on the controllability boundary (solid curves in the figure).

Next, in Figure 5, we fix ϵ^{-1} to 3 days (its average value for COVID-19) and we vary γ (the duration of the infectious period) in $\{2, 5, 8\}$ days. Note that we want to keep R_0 fixed, so we vary β accordingly. By keeping R_0

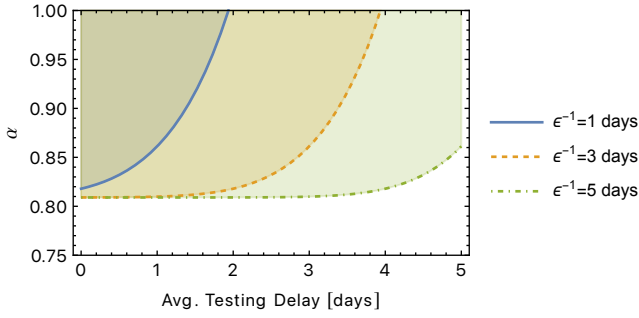


Fig. 4. Controllability when the average latent period increases (corresponding to ϵ decreasing). We consider $\epsilon^{-1} = \{1, 3, 5\}$ days. Control is attained in the shadowed regions.

constant we are basically saying that the epidemic is not more contagious as γ varies (because the contact process is adjusted to counterbalance its effect). The effect of varying R_0 is studied in the next paragraph. Again, the larger the contagious period, the easier the containment (Figure 5). Note that this result is due to the fixed R_0 , whereby each person, on average, infects the same number people in all three cases captured by Figure 5. With respect to the controllability boundary, a change in γ induces a change in the convexity of the boundary.

Finally, in Figure 6 we fix ϵ^{-1} and γ^{-1} (to their typical COVID-19 values of 3 and 2 days, respectively) and we change the R_0 of the epidemic by varying β . Note that this analysis is especially important, given the rise of novel variants with increased transmissibility (hence higher R_0). We study $R_0 \in \{2, 3, 4, 5, 6\}$. $R_0 = 2$ is the initial estimate for COVID-19 (original strain), then revised to be much higher in some areas (e.g. the estimate in [50] is $R_0 \sim 4$). The Alpha variant (B.1.1.7 lineage) is estimated to feature an at least 40% higher R [51] with respect to the original strain, while the Delta variant (B.1.617.2) has a transmissibility estimated between 6 and 7 [52], [53]. Note that the apparent even higher transmissibility of the recent Omicron variant (B.1.1.529) seems to be due to immune evasion (e.g., vaccines not as effective as for previous variants) rather than to an actual increase in basic transmissibility [54]. Figure 6 shows that, as expected, the impact of an increasing R_0 is much more disruptive than that of different latent/contagious windows. Specifically, even with instantaneous testing, the minimum uptake α increases as R_0 increases. This means that even a minimal fraction of untracked people can wreak havoc on the containment measures. In practice, though, with $R_0 = 4$, the control of the epidemic via digital contact tracing becomes impossible: an uptake above 95% is unrealistic for all the reasons discussed in Section I (e.g., technical problems with old smartphones, distrust by a fraction of the population). In this case, R_0 must be also brought down exploiting mitigation measures (social distancing, masks), in order to reduce the probability of infection upon contact, hence β .

VI. CONCLUSION

In this work, we have discussed the modelling efforts for COVID-19 and we have proposed a SEIR model that factors in digital contact tracing and is able to yield a closed-form

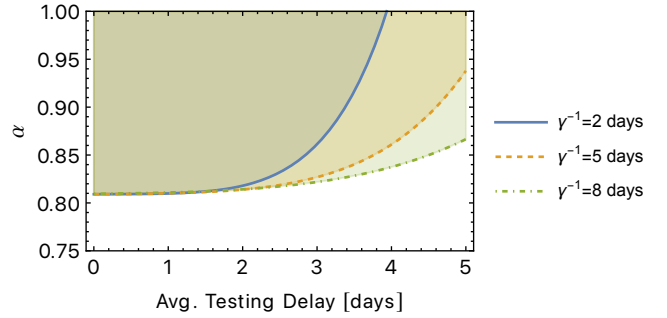


Fig. 5. Controllability when the average length of the contagious period increases (corresponding to γ decreasing). We consider $\gamma^{-1} = \{2, 5, 8\}$ days. Control is attained in the shadowed regions.

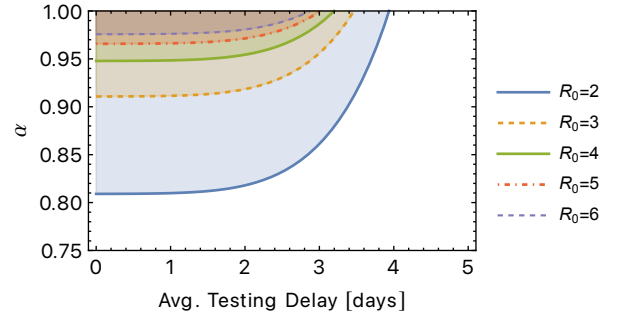


Fig. 6. Controllability when the $R_0 = \frac{\beta}{\gamma}$ increases (we fix γ and we increase β). We study $R_0 \in \{2, 3, 4, 5, 6\}$. Control is attained in the shadowed regions.

condition on the controllability of the epidemic. Leveraging this model, we have studied how the penetration of digital contact tracing apps within the population impacts the control of the epidemic. We have found that the penetration must be in general high, hence digital contact tracing may not be sufficient to contain an epidemic, even with fast turnaround of tests. Additional mitigation strategies, such as social distancing and mask-wearing, must be put in place. In addition, the impact of digital contact tracing is highest when the testing delay is low. If the test turnaround is greater than 4 days, digital contact tracing has zero impact on containment.

APPENDIX A PROOF OF THEOREM 1

Proof. We start by writing the ODE system corresponding to Figure 1:

$$\begin{aligned}
 \frac{dS_U}{dt} &= -\beta(1-\alpha)(I_U + I_T) \\
 \frac{dE_U}{dt} &= \beta(1-\alpha)(I_U + I_T) - \epsilon E_U \\
 \frac{dI_U}{dt} &= \epsilon E_U - \gamma I_U \\
 \frac{dS_T}{dt} &= -\beta\alpha(I_U + I_T) \\
 \frac{dE_T}{dt} &= \beta\alpha I_U + (\beta\alpha - \theta)I_T - \epsilon E_T \\
 \frac{dI_T}{dt} &= \epsilon E_T - (\gamma + \psi)I_T \\
 \frac{dR}{dt} &= \gamma I_U + (\gamma + \theta + \psi)I_T.
 \end{aligned} \tag{5}$$

The corresponding system of ODE can be re-written in matrix form as $\mathbf{y}' = \mathbf{A}\mathbf{y}$, where $\mathbf{y} = [E_U, I_U, E_T, I_T]^T$ and \mathbf{A} is given by the following:

$$\mathbf{A} = \begin{bmatrix} -\epsilon & \beta(1-\alpha) & 0 & \beta(1-\alpha) \\ \epsilon & -\gamma & 0 & 0 \\ 0 & \beta\alpha & -\epsilon & \beta\alpha - \theta \\ 0 & 0 & \epsilon & -\gamma - \psi \end{bmatrix}. \quad (6)$$

The system in (5) describes a dynamic system. Its stability (corresponding to the epidemic being under control or not) is assessed studying its eigenvalues (see, e.g., [50]), which correspond to the roots of the characteristic polynomial $p_A(x)$ of matrix \mathbf{A} . In fact, since the solutions to a system of linear ODE $\mathbf{y}' = \mathbf{A}\mathbf{y}$ are of the form $y(t) = \sum_i c_i * e^{r_i t}$ [55] (where c_i 's are constants and r_i 's the eigenvalues/roots), it is clear that a positive root introduces instability into the system, because there would be an exponential function with a positive argument, hence an exponential growth in the epidemic. We can thus study the roots of the characteristic polynomial $p_A(x)$ in order to assess under which conditions only negative roots exist. In order to avoid a trivial case, we assume $\beta > \gamma$ (i.e., the epidemic is not under control without contact tracing). Using Descartes' rule of signs, we can derive the number of positive and negative roots of $p_A(x)$ without needing to actually solve the polynomial (finding a closed-form for the roots would not be feasible in this case). Starting with the positive roots, we observe the following signs:

$$\{+, +, \text{sgn}(k_2), \text{sgn}(k_1), \text{sgn}(k_0)\}, \quad (7)$$

where we have expressed $p_A(x)$ as $\sum_i k_i x^i$, sgn is the sign function (where $\text{sgn}(\cdot) = 1$ corresponds to sign $+$, $\text{sgn}(\cdot) = -1$ corresponds to $-$), and k_2, k_1, k_0 are given by the following:

$$\begin{aligned} k_2 &= -\beta\epsilon + \epsilon^2 + \gamma(\gamma + \psi) + \epsilon(4\gamma + 2\psi + \theta), \\ k_1 &= \epsilon(2\gamma + \psi + \theta) + \\ &\quad + \gamma[2(\gamma + \psi) + \theta] - \beta(\epsilon + \gamma + \psi - \psi\alpha), \\ k_0 &= -[(\beta - \gamma)(\gamma + \psi + \theta)] + \beta(\psi + \theta)\alpha. \end{aligned} \quad (8)$$

By studying the functions $\text{sgn}(k_2), \text{sgn}(k_1), \text{sgn}(k_0)$, we obtain the following relationships between the coefficients' signs:

$$\text{sgn}(k_0) = 1 \Rightarrow \text{sgn}(k_1) = 1 \Rightarrow \text{sgn}(k_2) = 1. \quad (9)$$

In other words, since the rates must be all positive and $\alpha \in [0, 1]$, when coefficient k_0 is positive, k_2 and k_1 must be positive as well. This implies that not all possible sign permutations in Equation 7 are attainable, as illustrated in Table II. Discarding unattainable permutations, we can have at most one sign change across the coefficients of the polynomial, which implies at most one positive root. It thus follows that the condition under which we observe no sign changes is also the condition under which the epidemic can be controlled (zero positive roots). Thanks to Equation 9, we know that $\text{sgn}(k_0) = 1$ is a sufficient condition for this to happen. Then, solving for $k_0 > 0$ (with k_0 defined Equation 8), we obtain condition C1 in Equation 1.

TABLE II
ALL POSSIBLE SIGN PERMUTATIONS FOR THE COEFFICIENTS OF THE CHARACTERISTIC POLYNOMIAL OF \mathbf{A} . THE SHADOWED AREAS CORRESPOND TO UNFEASIBLE PERMUTATIONS.

k_4	k_3	k_2	k_1	k_0	sign changes
+	+	+	+	+	0
+	+	+	+	-	1
+	+	+	-	+	2
+	+	+	-	-	1
+	+	-	+	+	2
+	+	-	+	-	3
+	+	-	-	+	2
+	+	-	-	-	1

To conclude the proof, we just need to verify that there are no complex roots. This is easy to do by applying again Descartes' rule, this time to $p_A(-x)$. To this aim, we need to change the coefficient sign of odd-power terms (i.e., k_3, k_1) in Table II and count the sign changes. By summing the sign changes for positive and negative roots corresponding to the same permutation (equivalently, by summing the sign changes per corresponding row in Table II and Table II with the sign of odd-power terms changed), we obtain the total number of real roots. If we do the math, we discover that the total sign changes are at most 4, hence $p_A(x)$ features four real roots. Then, the number of complex roots is given by the difference between the degree of the polynomial and the maximum number of real roots. Since $p_A(x)$ is a polynomial of degree 4, we know that there are no complex roots. \square

REFERENCES

- [1] C. Fraser, S. Riley, R. M. Anderson, and N. M. Ferguson, "Factors that make an infectious disease outbreak controllable," *PNAS*, vol. 101, no. 16, pp. 6146–6151, 4 2004.
- [2] H. Cho, D. Ippolito, and Y. W. Yu, "Contact Tracing Mobile Apps for COVID-19: Privacy Considerations and Related Trade-offs," *arXiv*, 2020. [Online]. Available: <http://arxiv.org/abs/2003.11511>
- [3] R. Raskar, I. Schunemann, R. Barbar, K. Vilcans, J. Gray, P. Vepakomma, S. Kapa, A. Nuzzo, R. Gupta, A. Berke, D. Greenwood, C. Keegan, S. Kanaparti, R. Beaudry, D. Stansbury, B. B. Arcila, R. Kanaparti, V. Pamplona, F. M. Benedetti, A. Clough, R. Das, K. Jain, K. Louisy, G. Nadeau, V. Pamplona, S. Penrod, Y. Rajae, A. Singh, G. Storm, and J. Werner, "Apps Gone Rogue: Maintaining Personal Privacy in an Epidemic," *arXiv*, 2020. [Online]. Available: <http://arxiv.org/abs/2003.08567>
- [4] M. Nanni, G. Andrienko, A.-L. Barabási, C. Boldrini, F. Bonchi, C. Cattuto, F. Chiaromonte, G. Comandé, M. Conti, M. Coté, F. Dignum, V. Dignum, J. Domingo-Ferrer, P. Ferragina, F. Giannotti, R. Guidotti, D. Helbing, K. Kaski, J. Kertesz, S. Lehmann, B. Lepri, P. Lukowicz, S. Matwin, D. M. Jiménez, A. Monreale, K. Morik, N. Oliver, A. Passarella, A. Passerini, D. Pedreschi, A. Pentland, F. Pianesi, F. Pratesi, S. Rinzivillo, S. Ruggieri, A. Siebes, R. Trasarti, J. van den Hoven, and A. Vespignani, "Give more data, awareness and control to individual citizens, and they will help COVID-19 containment," *Transactions on Data Privacy*, vol. 13, no. 1, pp. 61–66, 2020.
- [5] N. Oliver, E. Letouzé, H. Sterly, S. Delataille, M. De Nadai, B. Lepri, R. Lambiotte, R. Benjamins, C. Cattuto, V. Colizza, N. de Cordes, S. P. Fraiberger, T. Koebé, S. Lehmann, J. Murillo, A. Pentland, P. N. Pham, F. Pivetta, A. A. Salah, J. Saramäki, S. V. Scarpino, M. Tizzoni, S. Verhulst, and P. Vinck, "Mobile phone data and COVID-19: Missing an opportunity?" *arXiv*, 2020. [Online]. Available: <http://arxiv.org/abs/2003.12347>

- [6] N. Ahmed, R. A. Michelin, W. Xue, S. Ruj, R. Malaney, S. S. Kanhere, A. Seneviratne, W. Hu, H. Janicke, and S. K. Jha, "A Survey of COVID-19 Contact Tracing Apps," pp. 134 577–134 601, 2020.
- [7] L. Ferretti, C. Wymant, M. Kendall, L. Zhao, A. Nurtay, L. Abeler-Dörner, M. Parker, D. Bonsall, and C. Fraser, "Quantifying SARS-CoV-2 transmission suggests epidemic control with digital contact tracing," *Science*, vol. 368, p. eabb6936, 2020.
- [8] T. Li, C. Cobb, Jackie, Yang, S. Baviskar, Y. Agarwal, B. Li, L. Bauer, and J. I. Hong, "What Makes People Install a COVID-19 Contact-Tracing App? Understanding the Influence of App Design and Individual Difference on Contact-Tracing App Adoption Intention," *Pervasive and Mobile Computing*, vol. 75, p. 101439, dec 2020. [Online]. Available: <http://arxiv.org/abs/2012.12415>
- [9] M. Conti, S. K. Das, C. Bisdikian, M. Kumar, L. M. Ni, A. Passarella, G. Roussos, G. Tröster, G. Tsudik, and F. Zambonelli, "Looking ahead in pervasive computing: Challenges and opportunities in the era of cyber-physical convergence," *Pervasive and Mobile Computing*, vol. 8, no. 1, pp. 2–21, 2012. [Online]. Available: <https://www.sciencedirect.com/science/article/pii/S1574119211001271>
- [10] V. Colizza, E. Grill, R. Mikolajczyk, C. Cattuto, A. Kucharski, S. Riley, M. Kendall, K. Lythgoe, D. Bonsall, C. Wymant, L. Abeler-Dörner, L. Ferretti, and C. Fraser, "Time to evaluate COVID-19 contact-tracing apps," pp. 361–362, mar 2021. [Online]. Available: <https://doi.org/10.1038/s41591-021-01237-5>
- [11] M. M. Böhmer, U. Buchholz, V. M. Corman, M. Hoch, K. Katz, D. V. Marosevic, S. Böhm, T. Woudenberg, N. Ackermann, R. Konrad, U. Eberle, B. Treis, A. Dangel, K. Bengs, V. Fingerle, A. Berger, S. Hörmansdorfer, S. Ippisch, B. Wicklein, A. Grahl, K. Pörtner, N. Müller, N. Zeitlmann, T. S. Boender, W. Cai, A. Reich, M. an der Heiden, U. Rexroth, O. Hamouda, J. Schneider, T. Veith, B. Mühlemann, R. Wölfel, M. Antwerpen, M. Walter, U. Protzer, B. Liebl, W. Haas, A. Sing, C. Drosten, and A. Zapf, "Investigation of a COVID-19 outbreak in Germany resulting from a single travel-associated primary case: a case series," *The Lancet Infectious Diseases*, 2020.
- [12] Z. Hu, C. Song, C. Xu, G. Jin, Y. Chen, X. Xu, H. Ma, W. Chen, Y. Lin, Y. Zheng, J. Wang, Z. Hu, Y. Yi, and H. Shen, "Clinical characteristics of 24 asymptomatic infections with COVID-19 screened among close contacts in Nanjing, China," *Science China Life Sciences*, 2020.
- [13] G. Qian, N. Yang, A. H. Y. Ma, L. Wang, G. Li, X. Chen, and X. Chen, "COVID-19 Transmission Within a Family Cluster by Presymptomatic Carriers in China," *Clinical infectious diseases : an official publication of the Infectious Diseases Society of America*, 2020.
- [14] C. Rothe, M. Schunk, P. Sothmann, G. Bretzel, G. Froeschl, C. Wallrauch, T. Zimmer, V. Thiel, C. Janke, W. Guggemos, M. Seilmaier, C. Drosten, P. Vollmar, K. Zwirgmaier, S. Zange, R. Wölfel, and M. Hoelscher, "Transmission of 2019-NCoV infection from an asymptomatic contact in Germany," 2020.
- [15] Y. Wang, J. Tong, Y. Qin, T. Xie, J. Li, J. Li, J. Xiang, Y. Cui, E. S. Higgs, J. Xiang, and Y. He, "Characterization of an asymptomatic cohort of SARS-CoV-2 infected individuals outside of Wuhan, China," *Clinical Infectious Diseases*, 2020.
- [16] P. Yu, J. Zhu, Z. Zhang, and Y. Han, "A familial cluster of infection associated with the 2019 novel coronavirus indicating possible person-to-person transmission during the incubation period," *Journal of Infectious Diseases*, 2020.
- [17] Y. Bai, L. Yao, T. Wei, F. Tian, D. Y. Jin, L. Chen, and M. Wang, "Presumed Asymptomatic Carrier Transmission of COVID-19," 2020.
- [18] W. E. Wei, Z. Li, C. J. Chiew, S. E. Yong, M. P. Toh, and V. J. Lee, "Presymptomatic Transmission of SARS-CoV-2 — Singapore, January 23–March 16, 2020," *MMWR. Morbidity and Mortality Weekly Report*, vol. 69, no. 14, 4 2020. [Online]. Available: http://www.cdc.gov/mmwr/volumes/69/wr/mm6914e1.htm?s_cid=mm6914e1_w
- [19] R. Wölfel, V. M. Corman, W. Guggemos, M. Seilmaier, S. Zange, M. A. Müller, D. Niemeyer, T. C. Jones, P. Vollmar, C. Rothe, M. Hoelscher, T. Bleicker, S. Brünink, J. Schneider, R. Ehmann, K. Zwirgmaier, C. Drosten, and C. Wendner, "Virological assessment of hospitalized patients with COVID-2019," *Nature*, pp. 1–10, 4 2020. [Online]. Available: http://www.nature.com/articles/s41586-020-2196-xhttps://www.technologyreview.com/s/615432/people-with-coronavirus-may-be-most-infectious-in-the-first-week-of-symptoms#?utm_medium=tr_social&utm_campaign=site_visitor.unpaid.engagement&utm_source=Twitter#Ec
- [20] A. Kimball, K. M. Hatfield, M. Arons, A. James, J. Taylor, K. Spicer, A. C. Bardossy, L. P. Oakley, S. Tanwar, Z. Chisty, J. M. Bell, M. Methner, J. Harney, J. R. Jacobs, C. M. Carlson, H. P. McLaughlin, N. Stone, S. Clark, C. Brostrom-Smith, L. C. Page, M. Kay, J. Lewis, D. Russell, B. Hiatt, J. Gant, J. S. Duchin, T. A. Clark, M. A. Honein, S. C. Reddy, J. A. Jernigan, A. Baer, L. M. Barnard, E. Benoliel, M. S. Fagalde, J. Ferro, H. G. Smith, E. Gonzales, N. Hatley, G. Hatt, M. Hope, M. Huntington-Frazier, V. Kawakami, J. L. Lenahan, M. D. Lukoff, E. B. Maier, S. McKeirnan, P. Montgomery, J. L. Morgan, L. A. Mummert, S. Pogosjans, F. X. Riedo, L. Schwarcz, D. Smith, S. Stearns, K. J. Sykes, H. Whitney, H. Ali, M. Banks, A. Balajee, E. J. Chow, B. Cooper, D. W. Currie, J. Dyal, J. Healy, M. Hughes, T. M. McMichael, L. Nolen, C. Olson, A. K. Rao, K. Schmit, N. G. Schwartz, F. Tobolowsky, R. Zacks, and S. Zane, "Asymptomatic and Presymptomatic SARS-CoV-2 Infections in Residents of a Long-Term Care Skilled Nursing Facility — King County, Washington, March 2020," *MMWR. Morbidity and Mortality Weekly Report*, vol. 69, no. 13, pp. 377–381, 4 2020. [Online]. Available: http://www.cdc.gov/mmwr/volumes/69/wr/mm6913e1.htm?s_cid=mm6913e1_w
- [21] R. Li, S. Pei, B. Chen, Y. Song, T. Zhang, W. Yang, and J. Shaman, "Substantial undocumented infection facilitates the rapid dissemination of novel coronavirus (SARS-CoV2)," *Science*, p. eabb3221, 3 2020.
- [22] Q. Li, X. Guan, P. Wu, X. Wang, L. Zhou, Y. Tong, R. Ren, K. S. Leung, E. H. Lau, J. Y. Wong, X. Xing, N. Xiang, Y. Wu, C. Li, Q. Chen, D. Li, T. Liu, J. Zhao, M. Liu, W. Tu, C. Chen, L. Jin, R. Yang, Q. Wang, S. Zhou, R. Wang, H. Liu, Y. Luo, Y. Liu, G. Shao, H. Li, Z. Tao, Y. Yang, Z. Deng, B. Liu, Z. Ma, Y. Zhang, G. Shi, T. T. Lam, J. T. Wu, G. F. Gao, B. J. Cowling, B. Yang, G. M. Leung, and Z. Feng, "Early Transmission Dynamics in Wuhan, China, of Novel Coronavirus-Infected Pneumonia," *New England Journal of Medicine*, vol. 382, no. 13, pp. 1199–1207, 3 2020. [Online]. Available: <http://www.nejm.org/doi/10.1056/NEJMoa2001316>
- [23] D. Sutton, K. Fuchs, M. D'Alton, and D. Goffman, "Universal Screening for SARS-CoV-2 in Women Admitted for Delivery," *New England Journal of Medicine*, p. NEJMc2009316, 4 2020. [Online]. Available: <http://www.nejm.org/doi/10.1056/NEJMc2009316>
- [24] X. He, E. H. Lau, P. Wu, X. Deng, J. Wang, X. Hao, Y. C. Lau, J. Y. Wong, Y. Guan, X. Tan, X. Mo, Y. Chen, B. Liao, W. Chen, F. Hu, Q. Zhang, M. Zhong, Y. Wu, L. Zhao, F. Zhang, B. J. Cowling, F. Li, and G. M. Leung, "Temporal dynamics in viral shedding and transmissibility of COVID-19," *medRxiv*, p. 2020.03.15.20036707, 3 2020. [Online]. Available: <https://www.medrxiv.org/content/10.1101/2020.03.15.20036707v2>
- [25] L. Luo, D. Liu, X.-l. Liao, X.-b. Wu, Q.-l. Jing, J.-z. Zheng, F.-h. Liu, S.-g. Yang, B. Bi, Z.-h. Li, J.-p. Liu, W.-q. Song, W. Zhu, Z.-h. Wang, X.-r. Zhang, P.-l. Chen, H.-m. Liu, X. Cheng, M.-c. Cai, Q.-m. Huang, P. Yang, X.-f. Yang, Z.-g. Huang, J.-l. Tang, Y. Ma, and C. Mao, "Modes of contact and risk of transmission in COVID-19 among close contacts," *medRxiv*, p. 2020.03.24.20042606, 3 2020.
- [26] L. Morawska and D. K. Milton, "It is Time to Address Airborne Transmission of COVID-19," *Clinical infectious diseases : an official publication of the Infectious Diseases Society of America*, 2020.
- [27] Z. Chagla, S. Hota, S. Khan, and D. Mertz, "Airborne Transmission of COVID-19," *Clinical Infectious Diseases*, 2020. [Online]. Available: <https://pubmed.ncbi.nlm.nih.gov/32780799/>
- [28] M. Klompas, M. A. Baker, and C. Rhee, "Airborne Transmission of SARS-CoV-2: Theoretical Considerations and Available Evidence," 2020.
- [29] M. Z. Bazant and J. W. Bush, "A guideline to limit indoor airborne transmission of COVID-19," *Proceedings of the National Academy of Sciences of the United States of America*, vol. 118, no. 17, apr 2021. [Online]. Available: <https://doi.org/10.1073/pnas.2018995118>
- [30] L. Bourouiba, "Turbulent Gas Clouds and Respiratory Pathogen Emissions: Potential Implications for Reducing Transmission of COVID-19," pp. E1–E2, 2020.
- [31] E. Hunter, B. M. Namee, and J. Kelleher, "An open-data-driven agent-based model to simulate infectious disease outbreaks," *PLoS ONE*, vol. 13, no. 12, p. e0208775, 12 2018. [Online]. Available: <http://dx.plos.org/10.1371/journal.pone.0208775>
- [32] S. Venkatramanan, B. Lewis, J. Chen, D. Higdon, A. Vullikanti, and M. Marathe, "Using data-driven agent-based models for forecasting emerging infectious diseases," *Epidemics*, vol. 22, pp. 43–49, 3 2018.
- [33] J. Hackl and T. Dubernet, "Epidemic spreading in urban areas using agent-based transportation models," *Future Internet*, vol. 11, no. 4, p. 92, 2019.
- [34] J. Parker and J. M. Epstein, "A distributed platform for global-scale agent-based models of disease transmission," *ACM Transactions on Modeling and Computer Simulation*, vol. 22, no. 1, 12 2011.
- [35] E. Bonabeau, "Agent-based modeling: Methods and techniques for simulating human systems," *Proceedings of the National Academy of Sciences of the United States of America*, vol. 99, no. SUPPL. 3, pp. 7280–7287, 5 2002.

- [36] J. J. Grefenstette, S. T. Brown, R. Rosenfeld, J. Depasse, N. T. Stone, P. C. Cooley, W. D. Wheaton, A. Fyshe, D. D. Galloway, A. Sriram, H. Guclu, T. Abraham, and D. S. Burke, "FRED (A Framework for Reconstructing Epidemic Dynamics): An open-source software system for modeling infectious diseases and control strategies using census-based populations," *BMC Public Health*, vol. 13, no. 1, pp. 1–14, 10 2013.
- [37] F. Liu, W. T. Enanoria, J. Zipprich, S. Blumberg, K. Harriman, S. F. Ackley, W. D. Wheaton, J. L. Allpress, and T. C. Porco, "The role of vaccination coverage, individual behaviors, and the public health response in the control of measles epidemics: An agent-based simulation for California," *BMC Public Health*, vol. 15, no. 1, pp. 1–16, 5 2015.
- [38] F. Brauer and C. Castillo-Chavez, *Mathematical Models in Population Biology and Epidemiology*. Springer, 2012.
- [39] G. Giordano, F. Blanchini, R. Bruno, P. Colaneri, A. Di Filippo, A. Di Matteo, and M. Colaneri, "Modelling the COVID-19 epidemic and implementation of population-wide interventions in Italy," *Nature medicine*, pp. 1–6, 4 2020.
- [40] J. Riou and C. L. Althaus, "Pattern of early human-to-human transmission of Wuhan 2019 novel coronavirus (2019-nCoV), December 2019 to January 2020," *Euro surveillance*, vol. 25, no. 4, 1 2020.
- [41] N. Ferguson, D. Laydon, G. Nedjati Gilani, N. Imai, K. Ainslie, M. Baguelin, S. Bhatia, A. Boonyasiri, Z. Cucunuba Perez, G. Cuomo-Dannenburg, and others, "Report 9: Impact of non-pharmaceutical interventions (NPIs) to reduce COVID19 mortality and healthcare demand," Imperial College London, Tech. Rep., 2020.
- [42] N. M. Linton, T. Kobayashi, Y. Yang, K. Hayashi, A. R. Akhmetzhanov, S.-m. Jung, B. Yuan, R. Kinoshita, and H. Nishiura, "Epidemiological characteristics of novel coronavirus infection: A statistical analysis of publicly available case data," *medRxiv*, 2020. [Online]. Available: <https://doi.org/10.1101/2020.01.26.20018754>
- [43] Q. Li, X. Guan, P. Wu, X. Wang, L. Zhou, Y. Tong, R. Ren, K. S. Leung, E. H. Lau, J. Y. Wong, X. Xing, N. Xiang, Y. Wu, C. Li, Q. Chen, D. Li, T. Liu, J. Zhao, M. Liu, W. Tu, C. Chen, L. Jin, R. Yang, Q. Wang, S. Zhou, R. Wang, H. Liu, Y. Luo, Y. Liu, G. Shao, H. Li, Z. Tao, Y. Yang, Z. Deng, B. Liu, Z. Ma, Y. Zhang, G. Shi, T. T. Lam, J. T. Wu, G. F. Gao, B. J. Cowling, B. Yang, G. M. Leung, and Z. Feng, "Early Transmission Dynamics in Wuhan, China, of Novel Coronavirus–Infected Pneumonia," *New England Journal of Medicine*, 1 2020.
- [44] I. Dorigatti, L. Okell, A. Cori, N. Imai, M. Baguelin, S. Bhatia, A. Boonyasiri, Z. Cucunubá, G. Cuomo-Dannenburg, R. Fitzjohn, H. Fu, K. Gaythorpe, A. Hamlet, W. Hinsley, N. Hong, M. Kwun, D. Laydon, G. Nedjati-Gilani, S. Riley, S. Van Elsland, E. Volz, H. Wang, R. Wang, C. Walters, X. Xi, C. Donnelly, A. Ghani, and N. Ferguson, "Report 4: Severity of 2019-novel coronavirus (nCoV)," Imperial College London, Tech. Rep., 2020. [Online]. Available: <https://doi.org/10.25561/77154>
- [45] A. Arenas, W. Cota, J. Gomez-Gardenes, S. Gomez, C. Granell, J. T. Matamalas, D. Soriano-Panos, and B. Steinegger, "Derivation of the effective reproduction number R for COVID-19 in relation to mobility restrictions and confinement," *medRxiv*, p. 2020.04.06.20054320, 2020.
- [46] D. J. Daley and J. Gani, *Epidemic modelling: an introduction*. Cambridge University Press, 1999.
- [47] F. M. Dekking, C. Kraaikamp, H. P. Lopuhaä, and L. E. Meester, *A Modern Introduction to Probability and Statistics: Understanding why and how*. Springer, 2005.
- [48] C. Boldrini, M. Conti, and A. Passarella, "From pareto inter-contact times to residuals," *IEEE communications letters*, vol. 15, no. 11, pp. 1256–1258, 2011.
- [49] Y. M. Bar-On, A. Flamholz, R. Phillips, and R. Milo, "Sars-cov-2 (Covid-19) by the numbers," *eLife*, 2020.
- [50] F. Casella, "Can the covid-19 epidemic be controlled on the basis of daily test reports?" *IEEE Control Systems Letters*, vol. 5, no. 3, pp. 1079–1084, 2020.
- [51] N. G. Davies, S. Abbott, R. C. Barnard, C. I. Jarvis, A. J. Kucharski, J. D. Munday, C. A. B. Pearson, T. W. Russell, D. C. Tully, A. D. Washburne, T. Wenseleers, A. Gimma, W. Waites, K. L. M. Wong, K. van Zandvoort, J. D. Silverman, K. Diaz-Ordaz, R. Keogh, R. M. Eggo, S. Funk, M. Jit, K. E. Atkins, and W. J. Edmunds, "Estimated transmissibility and impact of SARS-CoV-2 lineage B.1.1.7 in England," *Science*, vol. 372, no. 6538, p. eabg3055, apr 2021. [Online]. Available: <https://doi.org/10.1126/science.abg3055>
- [52] R. Pung, T. Minn Mak, C. Covid, working Group, A. J. Kucharski, and V. J. Lee, "Serial intervals observed in SARS-CoV-2 B.1.617.2 variant cases," *medRxiv*, p. 2021.06.04.21258205, jun 2021. [Online]. Available: <https://doi.org/10.1101/2021.06.04.21258205>
- [53] J. Dagpunar, "Interim estimates of increased transmissibility, growth rate, and reproduction number of the Covid-19 B.1.617.2 variant of concern in the United Kingdom," *medRxiv*, p. 2021.06.03.21258293, jun 2021. [Online]. Available: <https://doi.org/10.1101/2021.06.03.21258293>
- [54] F. P. Lyngse, L. H. Mortensen, M. J. Denwood, L. E. Christiansen, C. H. Møller, R. L. Skov, K. Spiess, A. Fomsgaard, M. M. Lassaunière, M. Rasmussen, M. Stegger, C. Nielsen, R. N. Sieber, A. S. Cohen, F. T. Møller, M. Overvad, K. Mølbak, T. G. Krause, and C. T. Kirkeby, "Sars-cov-2 omicron voc transmission in danish households," *medRxiv*, 2021. [Online]. Available: <https://www.medrxiv.org/content/early/2021/12/27/2021.12.27.21268278>
- [55] M. Braun, *Differential Equations and Their Applications An Introduction to Applied Mathematics*. Springer, 1993.